applied sciences

MDPI

Article

Separation of Albumin from Bovine Serum Applying Ionic-Liquid-Based Aqueous Biphasic Systems

Ana F. C. S. Rufino [1], Mafalda R. Almeida [1], Mukesh Sharma [2], João A. P. Coutinho [1] and Mara G. Freire [1,*]

[1] Department of Chemistry, CICECO-Aveiro Institute of Materials, University of Aveiro, 3810-193 Aveiro, Portugal; anafiliparufino@ua.pt (A.F.C.S.R.); mafalda.almeida@ua.pt (M.R.A.); jcoutinho@ua.pt (J.A.P.C.)

[2] Indian Center for Climate & Societal Impacts Research (ICCSIR), VRTI-Campus, Nagalpur Road, Mandvi, Kachchh, Gujarat 370 465, India; sharma.mukesh094@gmail.com

* Correspondence: maragfreire@ua.pt

Abstract: In this work, the extraction and separation of bovine serum albumin (BSA) from its original matrix, i.e., bovine serum, was performed using a novel ionic-liquid-based aqueous biphasic system (IL-based ABS). To this end, imidazolium-, phosphonium-, and ammonium-based ILs, combined with the anions' acetate, arginate and derived from Good Buffers, were synthesized, characterized, and applied in the development of ABS with K_2HPO_4/KH_2PO_4 buffer aqueous solutions at pH 7. Initial studies with commercial BSA revealed a preferential migration of the protein to the IL-rich phase, with extraction efficiencies of 100% obtained in a single-step. BSA recovery yields ranging between 64.0% and 84.9% were achieved, with the system comprising the IL tetrabutylammonium acetate leading to the maximum recovery yield. With this IL, BSA was directly extracted and separated from bovine serum using the respective ABS. Different serum dilutions were further investigated to improve the separation performance. Under the best identified conditions, BSA can be extracted from bovine serum with a recovery yield of 85.6% and a purity of 61.2%. Moreover, it is shown that the BSA secondary structure is maintained in the extraction process, i.e., after being extracted to the IL-rich phase. Overall, the new ABS herein proposed may be used as an alternative platform for the purification of BSA from serum samples and can be applied to other added-value proteins.

Keywords: aqueous biphasic systems; ionic liquids; proteins; purification; bovine serum; bovine serum albumin

Citation: Rufino, A.F.C.S.; Almeida, M.R.; Sharma, M.; Coutinho, J.A.P.; Freire, M.G. Separation of Albumin from Bovine Serum Applying Ionic-Liquid-Based Aqueous Biphasic Systems. *Appl. Sci.* **2022**, *12*, 707. https://doi.org/10.3390/app12020707

Academic Editor: Laura Lomba Eraso

Received: 10 November 2021
Accepted: 5 January 2022
Published: 11 January 2022

1. Introduction

Proteins play a fundamental role in biological processes and have high value in different industrial applications, e.g., in the food, biopharmaceutical or cosmetic industries [1]. Conventional techniques for proteins separation and purification include chromatography, electrophoresis, precipitation, and filtration-related techniques, among others [2]. However, there is a need of finding more cost-effective techniques to efficiently separate and purify proteins, while being capable of maintaining their native structure and function/activity [3]. Aqueous biphasic systems (ABS) have been proposed as an alternative technique to separate and purify proteins, mainly due to their versatility and biocompatible character if properly designed [4].

ABS are formed by the dissolution of at least two water-soluble solutes (typically two polymers, a polymer and a salt, or two salts) in aqueous media [5], above which, in certain concentrations, there is phase separation. Conventional polymer-based ABS have been applied in the extraction and purification of several biological compounds and materials, such as cells [6], nucleic acids [7], amino acids [8], proteins, antibodies [9], and enzymes [10–12]. However, the coexisting phases in typical polymer-based ABS present a limited polarity difference, preventing high extraction efficiencies and selectivities to be achieved in a single-step [13]. Ionic-liquid-based (IL-based) ABS were later proposed

as an alternative to polymer-based ABS, with numerous advantages [14]. These ABS are less viscous, show faster phase separation rates, and generally lead to higher extraction efficiencies. ILs are salts with lower melting temperatures than conventional salts, being constituted by an organic cation and an organic or inorganic anion [15]. Most ILs present a negligible volatility at atmospheric conditions, high thermal and chemical stabilities, a strong solvation capability for a large variety of compounds, and present the ability to conjugate ions according to the intended application, being usually described as "designer solvents" [16].

To improve the biocompatible character of ILs to be applied in ABS, the IL anion can be selected according to the desired application. IL anions derived from biological buffers (Good-Buffer's (GB)-ILs) [17–19], amino acids [20], and carboxylic acids [21] have been applied in the extraction and separation of amino acids and proteins. However, most ILs reported in the literature were combined with imidazolium cations [22,23], which may compromise their biocompatibility. On the other hand, the use of ammonium- and phosphonium-based ILs have been reported for the extraction of some proteins, such as ovalbumin and lysozyme [24]. Aiming at identifying the best cation–anion combinations of ILs to form ABS, in this work, ILs combining the imidazolium-, phosphonium-, and tetraalkylammonium cations, and the acetate, arginate, and Good-Buffer-based anions, were synthesized, characterized, and used in the creation of IL-based ABS. These systems were then studied as separation platforms of bovine serum albumin (BSA). BSA was studied as the target protein due to its relevance in pharmaceutical studies [25] and due to their presence in bovine serum as a biological and complex medium from which it needs to be isolated.

2. Materials and Methods

2.1. Chemicals and Reagents

Several ILs were synthesized by us, namely tetrabutylphosphonium arginate ($[P_{4444}][Arg]$), tetrabutylammonium arginate ($[N_{4444}][Arg]$), tetrabutylphosphonium 2-(N-morpholino)ethanesulfonate ($[P_{4444}][MES]$), tetrabutylammonium 2-(N-morpholino) ethanesulfonate ($[N_{4444}][MES]$), 1-butyl-3-methylimidazolium 2-(N-morpholino)ethanesulfonate ($[C_4mim][MES]$), tetrabutylphosphonium acetate ($[P_{4444}][Ac]$), and tetrabutylammonium acetate ($[N_{4444}][Ac]$), according to previously reported protocols [17,19,26,27]. Details on the ILs synthesis are given in the Supporting Information (SI). The purity of all ILs were checked by ^1H and ^{13}C nuclear magnetic resonance (NMR), being >95%. The ILs synthesized are solid at room temperature and completely water-soluble. The IL 1-butyl-3-methylimidazolium acetate ($[C_4mim][Ac]$, 97% purity, was acquired from Iolitec. The chemical structures of the studied ILs are presented in Figure 1.

The salts used for the buffer solution preparation were potassium phosphate dibasic trihydrate ($K_2HPO_4 \cdot 3H_2O$, extra-pure) from Panreac, and potassium phosphate monobasic (KH_2PO_4, extra-pure) acquired from Fisher Chemical. Phosphate Buffered Saline (PBS) pellets (pH = 7.4) were acquired from Sigma.

BSA (purity $\geq$ 96%), IgG (purity $\geq$ 98%) and bovine serum were acquired from Fischer Scientific, Innovative Research and Merck, respectively. All aqueous solutions were prepared with distilled water.

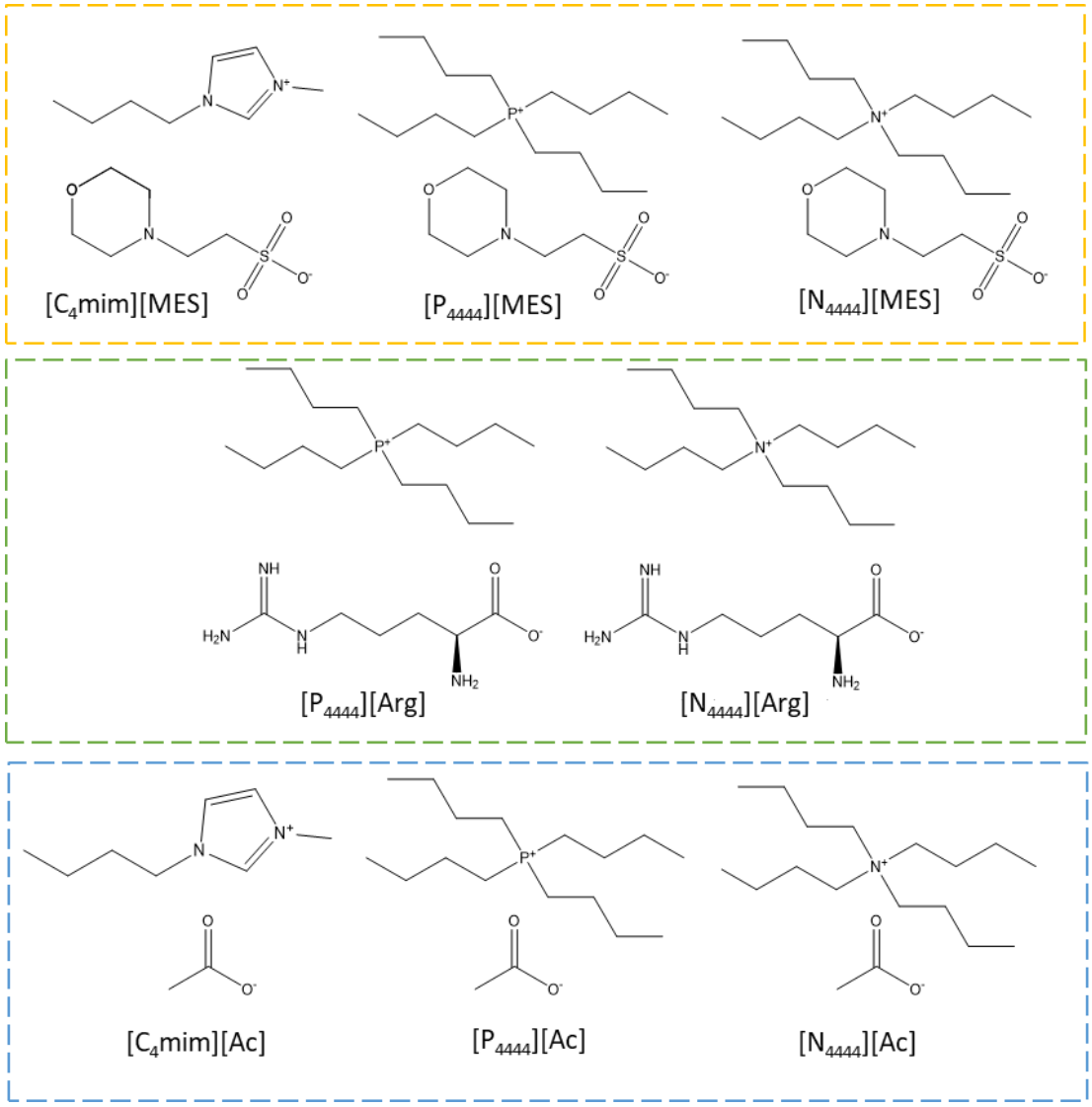

Figure 1. Chemical structures of the ionic liquids investigated.

2.2. Determination of ABS Phase Diagrams

The ABS phase diagrams for the systems composed of each IL and K_2HPO_4/KH_2PO_4 buffer at pH 7 were determined at 25 (±1) °C and atmospheric pressure, allowing to define the conditions under which it is possible to obtain a two-phase system to be applied in the extraction process. The binodal curves were determined using the cloud point titration method [28]. IL aqueous solutions with concentrations ranging from 40 to 60 wt% were prepared. To these solutions, an aqueous solution of 40 wt% K_2HPO_4/KH_2PO_4 buffer at pH 7 was added, allowing the identification of a cloud point corresponding to the biphasic regime, followed by the addition of water until the identification of clear solutions, corresponding to the monophasic regime. Further details on the ABS determination/characterization can be found elsewhere [29].

The experimental binodal curves were adjusted by the equation proposed by Merchuk et al. [30]:

$$[IL] = A.e^{B.[salt]^{0.5} - C.[salt]^3} \quad (1)$$

where (*IL*) and (*salt*) correspond to the IL and salt weight fraction percentages, respectively, and the coefficients *A*, *B*, and *C* are fitting parameters determined by the regression of the experimental data. The composition of each phase at given mixture compositions, i.e.,

the respective tie-lengths (TLs), as well as the corresponding tie-line lengths (TLLs), were additionally determined. Details for their determination are provided in the Supporting Information (Tables S1–S5).

2.3. Extraction and Purification of BSA

Initial studies were carried out with the pure protein (BSA). ABS were prepared with 35 wt% of each IL, 20 wt% of K_2HPO_4/KH_2PO_4 buffer at pH 7, and 45 wt% of BSA aqueous solution at 2 g·L^{-1} in deionized water. This mixture point was selected according to the phase diagrams determination, fitting within the biphasic region of all studied ABSs. The obtained mixtures were stirred and centrifuged for 10 min at 10,000 rpm, and left to equilibrate for 15 min at 25 (±1) °C. The two phases were carefully separated and used in several analysis to evaluate the ABS performance on the BSA extraction and separation from the serum samples. For the purification studies of BSA from bovine serum, dilutions of 1:25, 1:20, 1:15, and 1:10 (*v:v*) of bovine serum in distilled water were prepared and added to the ABS preparations (45 wt%). For all systems, the IL-rich phase corresponds to the top phase, while the salt-rich phase corresponds to the bottom phase.

BSA and the remaining proteins present in serum bovine were quantified in each ABS phase by size-exclusion high-performance liquid chromatography (SE-HPLC). The samples were diluted at a 1:10 (*v:v*) ratio with phosphate buffer (50 mmol·L^{-1} phosphate buffer pH 7.0 with NaCl 0.3 mol·L^{-1}) used as the mobile phase for quantification. The equipment used was a Chromaster HPLC system (VWR Hitachi) equipped with a binary pump, column oven (40 °C), temperature controlled auto-sampler (10 °C), DAD detector and an analytical column Shodex Protein KW- 802.5 (8 mm × 300 mm). A 50 mmol·L^{-1} phosphate buffer pH 7.0 with NaCl 0.3 mol·L^{-1} was run isocratically with a flow rate of 0.5 mL·min^{-1} and the injection volume was of 25 µL. The wavelength was set at 280 nm with a total analysis time of 40 min and the retention time of BSA was found to be ca. 16.5 min. The calibration curve was established with BSA from 0.05 to 7.00 g·L^{-1}. The ABS performance was evaluated in terms of extraction efficiency, yield, and purity for BSA, using three replicates.

The extraction efficiency of the studied systems for BSA, *EE*%, was determined according to the following equation:

$$EE\% = \frac{w_{\mathrm{BSA}}^{IL}}{w_{\mathrm{BSA}}^{salt} + w_{\mathrm{BSA}}^{IL}} \times 100 \quad (2)$$

where w_{BSA}^{IL}, w_{BSA}^{salt} represent the BSA total weight in the IL-rich and salt-rich phases, respectively.

The extraction yield of BSA (*Yield%)* was determined according to the following equation:

$$Yield\% = \frac{w_{\mathrm{BSA}}^{IL}}{w_{\mathrm{BSA}_{\mathrm{initial/Serum}}}} \times 100 \quad (3)$$

where $w_{\mathrm{BSA}_{\mathrm{initial/serum}}}$ represents the weight of BSA added to the system and w_{BSA}^{IL} the weight of BSA in the IL-rich phase.

The purity of BSA was calculated dividing the HPLC peak area of BSA (A_{BSA}) by the total area of the peaks corresponding to all proteins present in the phases of the different systems $A_{totalprotein}$, according the following equation:

$$Purity\% = \frac{A_{\mathrm{BSA}}}{A_{totalprotein}} \times 100 \quad (4)$$

2.4. SDS-PAGE and Circular Dichroism

The protein profile of bovine serum and of the IL-rich phase after an ultrafiltration (UF) step was evaluated by sodium dodecyl sulphate polyacrylamide gel electrophoresis (SDS-PAGE) using an Amersham ECLTM Gel from GE Healthcare Life Sciences. For the analysis of the IL-rich phase an UF step was performed to remove the IL and respective

interferences, dissolving the retentate in PBS buffer for the analysis. Samples were mixed with the sample buffer 1:1 (*v:v*), consisting of: 2.5 mL of 0.5 M Tris-HCl pH 6.8, 12.0 mL of glycerol, 4.0 mL of 10% (*w/v*) SDS, 2.0 mg of bromophenol blue and 310 mg of dithiothreitol (DTT); and heated for denaturation at (95 ± 1) °C for 5 min. Electrophoresis was run on polyacrylamide gels 4–20% at 105 V for 90 min. The running buffer used was Tris-Tricine-SDS Buffer 10×x (1.0 M Tris, 1.0 M Tricine, 10% SDS, pH 8.3). The gel was stained with Coomassie Brilliant Blue G-250. A molecular weight full-range marker (VWR) was used as protein standards.

To evaluate the maintenance of the BSA secondary structure after the extraction step and UF applied to the IL-rich phase, circular dichroism (CD) was applied. The analysis of pure BSA and of the IL-rich phase after the UF step was performed by CD spectroscopy (JASCO-1500), with three spectra recorded consecutively with a 1 mm path length quartz cuvette and the parameters: 100 nm per minute, at 20 °C cell temperature, response time and bandwidth were 2 s and 0.2 nm, respectively. The baseline was established with a phosphate-buffered saline (PBS) solution. The secondary structure content of BSA was calculated using DichroWeb with the Analysis Program CDSSTR and the reference set 4 (optimized for the range 190–240 nm) [31].

3. Results and Discussion

3.1. ABS Phase Diagrams

All the ABS under study, composed of IL + K_2HPO_4/KH_2PO_4 buffer at pH 7 + water, were characterized by obtaining their phase diagrams at 25 (±1) °C and atmospheric pressure. The selection of the salt and pH was made with the goal of keeping the biological activity and native structure of proteins [29], in this case BSA. All the ILs under study were able to form ABS when mixed with K_2HPO_4/KH_2PO_4 buffer at pH 7, for which the corresponding binodal curves are shown in Figure 2. The data related to the experimental weight fraction of binodal curves are presented in the Supporting Information, Tables S1–S8, whereas the data related to TLs, TLLs, and fitting parameters of Equation (1) are provided in Tables S9 and S10. The results in Figure 2 are provided in weight fraction, thus not taking into account the molecular weight of the IL, due to their relevance from a biotechnological application perspective.

The larger the biphasic region, i.e., the region above each solubility curve, the higher is the facility to form two aqueous phases. Therefore, the studied ILs can be ordered according to their increasing order of ABS forming ability, which at 20 wt% of salt (Figure 2) is as follows: $[P_{4444}][Ac] \approx [N_{4444}][MES] < [P_{4444}][Arg] < [N_{4444}][Ac] \approx [N_{4444}][Arg] < [C_4mim][MES] \approx [P_{4444}][MES] < [C_4mim][Ac]$. Although a trend is here depicted, it should be mentioned that the phase diagrams almost totally overlap with very small differences between them, meaning that no major differences exist in the ILs ability to create ABS with the studied salt (K_2HPO_4/KH_2PO_4) when evaluating their ranking in weight fraction. The ILs ranking in terms of molality units can be appraised in the Supporting Information, Figure S15, for which the related molecular-level mechanisms have been previously reported and discussed [32,33]. Overall, the formation of ABS composed of ILs and salts is favored with the increase in the IL hydrophobicity or its affinity for water, so that a stronger salting-out effect exerted by the inorganic salts occurs.

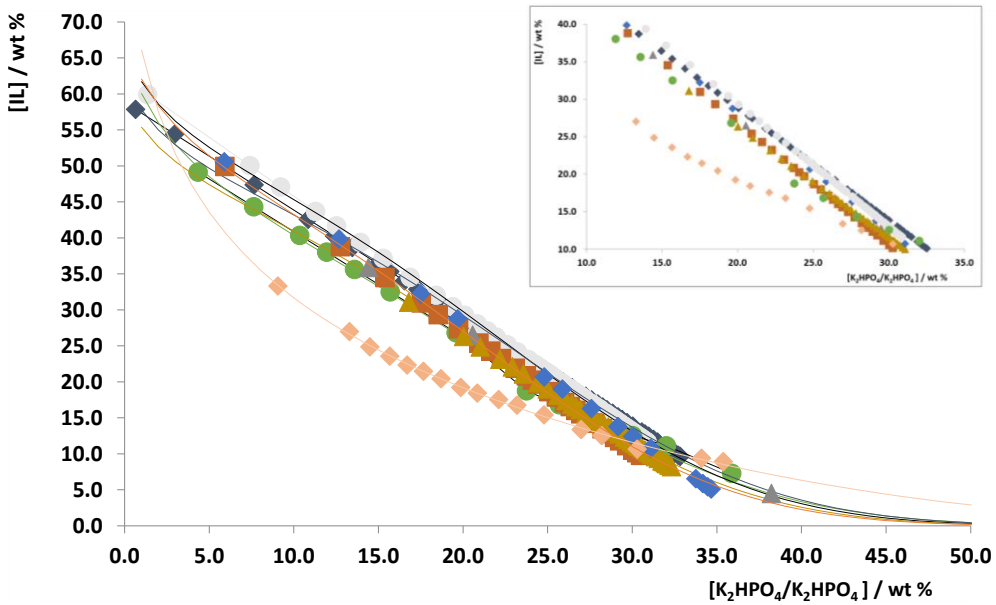

Figure 2. Phase diagrams for the systems composed of ionic liquid + K_2HPO_4/KH_2PO_4 buffer at pH 7 + H_2O at 25 °C: (C_4mim][MES] (●); [N_{4444}][MES] (♦); [P_{4444}][MES] (▲); [N_{4444}][Arg] (▲); [P_{4444}][Arg] (♦); [C_4mim][Ac] (♦); [N_{4444}][Ac] (■); [P_{4444}][Ac] (●). The solid lines represent the fitting by Equation (1). The insert graph presents a zoom-in of the phase diagrams to better allow the visualization of the mixture point used in the extraction of BSA: 35 wt% of IL + 20 wt% K_2HPO_4/KH_2PO_4 buffer at pH 7.

3.2. Extraction and Purification of BSA

After the characterization of the investigated ABS, they were applied to extract BSA and then to purify this protein from bovine serum. To this end, a common ABS mixture point was used: 35 wt% of IL + 20 wt% K_2HPO_4/KH_2PO_4 buffer at pH 7 + 45 wt% aqueous solution of BSA/bovine serum. The extraction efficiency (*EE*%), yield and purity of BSA were obtained by the quantification of BSA and remaining proteins by SE-HPLC. Overall, six out of the eight ILs investigated allowed the partition of the protein in a two-phase system, namely, [C_4mim][MES], [N_{4444}][MES], [P_{4444}][MES], [C_4mim][Ac], [N_{4444}][Ac], and [P_{4444}][Ac]. The arginate-based-ILs, namely, [N_{4444}][Arg] and [P_{4444}][Arg], lead to the complete precipitation of the protein in the bottom of the system and did not allow the formation of a liquid–liquid system when in presence of the protein solution. This result shows that relevant interactions between the IL arginate anion and the serum constituents occur, not allowing the creation of ABS.

In the studied systems that form an ABS in presence of BSA, the protein preferentially partitions to the top phase (IL-rich phase), in agreement with data reported for ABS composed of other ILs and K_2HPO_4/KH_2PO_4 buffer for other enzymes and proteins, as well as for BSA [34–37]. This behavior is the result of the salting-out effect provided by the phosphate buffer, thus improving the migration of the proteins to the opposite phase, combined with favorable interactions that may be established between the IL and BSA. These could correspond to hydrogen-bonding, or electrostatic and hydrophobic interactions [36,38–40]. In the current work, BSA is negatively charged (isoeletric point (pI) = 4.5–4.9) [41,42] at the pH at which ABSs were formed, and electrostatic interactions may be established.

The extraction efficiencies and yield of the assays carried out with pure BSA are given in Figure 3, with the detailed data provided in the Supporting Information (Table S11). Figure 3 allows comparing the performance of the IL-based ABS under study in terms of extraction efficiency and extractionyield of BSA, allowing the identification of the best system to be used in the next step of the work, i.e., in the separation of BSA from bovine serum albumin. In all ABS, the extraction efficiency of BSA to the IL-rich phase is 100%, whereas the extraction yield values range from 43.7% to 84.9%. The system

constituted by [C_4mim][Ac] presents the lowest yield (43.7%), whereas those composed of [N_{4444}][Ac] and [P_{4444}][Ac] lead to the highest yields, 84.9% and 82.9%, respectively. This set of results show that there is a significant loss of protein stability with systems comprising imidazolium-based ILs; although, these are still the most investigated class of ILs in the field of separations. The denaturation of BSA by imidazolium-based ILs has been previously reported, with loss of secondary and tertiary structure, and results from hydrophobic and electrostatic established between BSA and the IL [43]. On the other hand, quaternary ammonium-based ILs have been reported as protein stabilizers [44], supporting the results here observed and reinforcing their study in protein separation studies. ABS comprising cholinium-based ILs have been also reported for the extraction for BSA in an attempt to use more biocompatible ILs and maintain the protein structure [45].

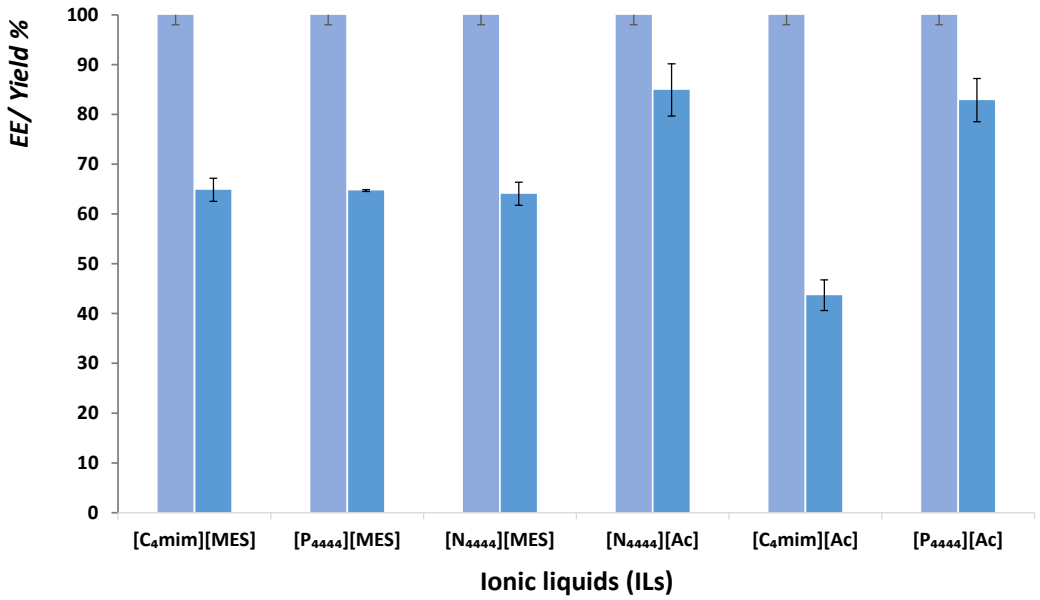

Figure 3. Extraction efficiencies *(EE%)* (■) and yield (*Yield%*) (■) of bovine serum albumin in the ionic-liquid-rich phase of the studied aqueous biphasic systems composed of 35 wt% of ionic liquid + 20 wt% K_2HPO_4/KH_2PO_4 buffer at pH 7.

Extraction efficiencies up to 100% for pure BSA with IL-based ABS have been described with systems constituted by cholinium-based ILs + polymer (PPG 400) and phosphonium- and ammonium-based ILs + potassium citrate/citric acid at pH 7, being the reported results [18,46] similar to those obtained in this work. On the other hand, ABS with cholinium-based ILs combined with amino acids and polymers (polyethylene glycol di-methyl ether 250 and/or PPG, respectively) lead to lower extraction efficiencies, namely, 82.75%, 91.6%, and 85.91% under the best conditions [45,47,48], reinforcing the relevance of employing inorganic salts when high extraction efficiencies in IL-based ABS are aimed. Additionally, imidazolium-based systems combined with K_2HPO_4 led to BSA extraction efficiencies of 82.7–100.7%, but with no extraction yields reported [49].

Regarding the different anions effect it is shown that ABS with the ILs based on the acetate anion lead to the maximum and minimum extraction yields, with the ABS comprising [N_{4444}]Ac and [P_{4444}][Ac] presenting the maximum values, and that constituted by [C_4mim][Ac] to the minimum extraction yield. Although no differences are shown in the extraction efficiencies, these results clearly show that the cation effect has a higher impact in the BSA extraction yield, which may be related to the fact of having BSA as a negatively charged protein at the studied pH. Furthermore, these results seem to indicate that IL cations are the species that position themselves closer to the proteins, which is explained by the preferential hydrogen-bonded network established between the IL anions and water in the bulk phase [50]. These results, showing a higher effect of the IL cation,

are in agreement with the literature, where it has been shown that the concentration of IL cations is higher than that of anions at the protein surface, regardless of the protein charge [51–53]. Overall, these results reinforce the need of further investigating new ABS with quaternary ammonium- and phosphonium-based ILs, while also reducing their cost and toxicity when compared to imidazolium-based ILs [54–56].

Due to its higher extraction yield, thus corresponding to lower losses of BSA, the ABS composed of the IL [N_{4444}][Ac] was chosen to extract BSA from the real sample, i.e., bovine serum. Using the same mixture point (35 wt% of IL + 20 wt% K_2HPO_4/KH_2PO_4 buffer at pH 7 + 45 wt% bovine serum), four dilutions (1:25,1:20,1:15,1:10 *v:v*) of bovine serum were tested, whose results are given in Figure 4. These experiments are relevant to appraise the protein saturation and possible proteins aggregation/precipitation phenomena. The higher the dilution of serum, the higher is the BSA extraction yield, ranging from 61.0 to 100.0%, thus reflecting the relevance of the IL-rich phase saturation. Detailed results are provided in the Supporting Information, Table S12. On the other hand, an opposite, yet slight, trend is observed when addressing the BSA purity. In this case, values between 51.9% and 61.2% are achieved, with the highest value found for the serum dilution corresponding to 1:15 (*v:v*). These results indicate that there is a competition for the proteins dissolution in the IL-rich phase and respective phase saturation, while considering that immunoglobulin G (IgG) is the second highest abundant protein in bovine serum, which should partition to the opposite phase, or be precipitated to allow higher purity levels of BSA. In summary, the best results were obtained with the ABS composed of [N_{4444}][Ac], with a serum dilution of 1:15 (*v:v*), in which an extraction yield of BSA of 85.6% and purity of 61.2% were achieved in one step.

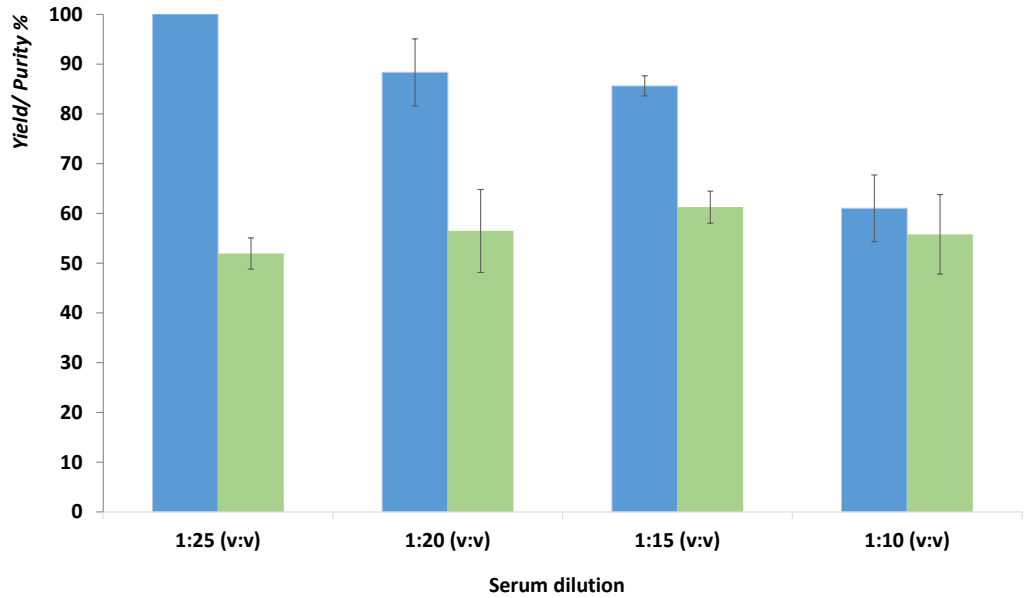

Figure 4. Extraction yield (*Yield%*) (■) and purity (*Purity%*) (■) of bovine serum albumin in the ionic-liquid-rich phase extracted from bovine serum with the aqueous biphasic systems comprising [N_{4444}][Ac] as function of the bovine serum dilution.

The first large-scale technique for separating blood components was developed in the 1940–1950s by Cohn and co-workers, corresponding to Fractional Extraction [57,58]. Up to date, several methods have been developed combining this method resorting to fractionation with ethyl alcohol and other techniques, such as ionic exchange and affinity chromatography. This fractionation step coupled to chromatography allows BSA with a purity of 99% to be obtained [59–61]. In addition to these methods, other combinations, such as precipitation with ammonium sulfate combined with liquid chromatography [62], and the use of ion exchange [63], affinity [64,65], and simulated moving bed (SMB) [66]

chromatography without previous precipitation/fractionation steps, have been reported, resulting in BSA with a purity higher than 90%. In addition to these well-developed techniques, steric exclusion chromatography with a cryogel column has been more recently reported, with purity values of 26.9% in the elution fraction and 103% in the breakthrough fraction [67]. Although our IL-based ABSs do not allow purification levels higher than 90% as the ones here described, it should be remarked that the purity of 61.2% of BSA was achieved in a single-step, i.e., directly from bovine serum without previous fractionation steps. On the other hand, no chromatographic steps are applied. If higher purification levels are required, IL-based ABSs need to be further optimized, in terms of composition, or applied under continuous mode to allow several stages of equilibrium [68]. These could also be combined with other strategies such as chromatography, ultrafiltration, or induced precipitation [69].

SE-HPLC was used to quantify BSA; however, this technique also permits obtaining information about the occurrence of protein aggregates or proteins fragmentation, thus allowing the confirmation that BSA stability is maintained throughout the extraction process in the IL-rich phase (an example of a SE-HPLC chromatogram is provided in Figure S16 in the Supporting Information). The protein profile of the IL-rich phase of the ABS comprising [N_{4444}][Ac was evaluated by SDS-PAGE, being given in Figure 5A. Results show that bovine serum is mainly composed of IgG and BSA. After the extraction with ABS, a decrease in the IgG content is visible (as appraised by the intensity of the respective heavy and light chain bands), thus leading to an increase in the purity of BSA in the IL-rich phase.

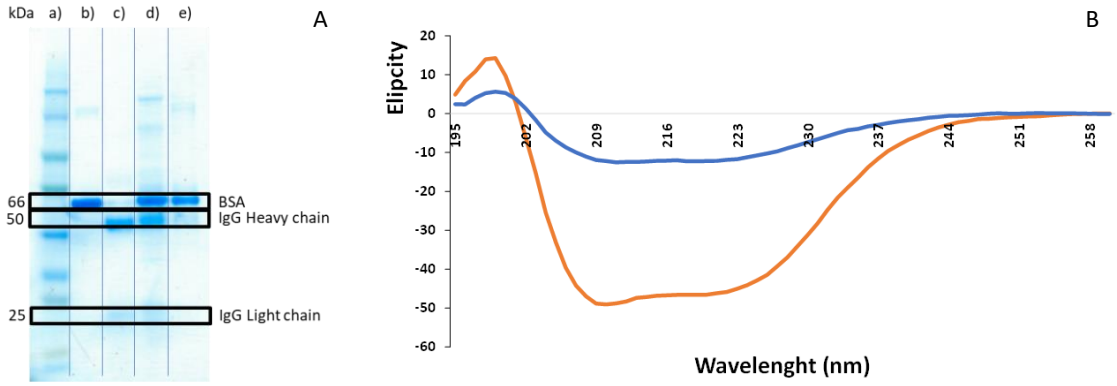

Figure 5. (**A**)—SDS-Page gel analysis of (a) Molecular weight marker, (b) Bovine serum albumin, (c) Immunoglobulin G, (d) Bovine Serum diluted at 1:100 (*v:v*), (e) Ionic-liquid-rich phase of the [N_{4444}][Ac] system after an ultrafiltration step, with Bovine serum albumin and Immunoglobulin G chains identified; (**B**)—Circular dichroism analysis to evaluate the Bovine serum albumin secondary structure stability in the ionic-liquid-rich phase (—) and pure Bovine serum albumin at 0.25 mg.mL^{-1} (—).

Finally, and to ensure the protein stability after the extraction step and in the IL-rich phase, CD spectroscopy was applied, whose spectra are depicted in Figure 5B. CD spectra allow the secondary structure of proteins to be assessed and their conformation in α-helix, β-sheet, β-turn, and random coils to be analyzed [70]. Below 240 nm peptide bonds can be observed, while aromatic amino acid side chains and disulfide bonds can be analyzed in the range 260–320 nm and close to 260 nm, respectively. In the case of pure BSA, a protein profile with a rich α-helix structure is presented, with two minimums occurring at approximately 209 nm and 222 nm and with a maximum between 190 and 195 nm [70,71]. When comparing the spectra of pure BSA and of BSA after the extraction step to the IL-rich phase, the shape of the two spectra is highly similar, suggesting the maintenance of the secondary structure of BSA in the IL-rich phase after the extraction step. The composition of the BSA secondary structure is mostly α-helix (62%), with a lower content in β-sheets (7%), turns (12%), and random coils (19%) [72,73]. The values obtained in this work for BSA in PBS aqueous solutions are very similar for the α-helix

content (64%), with a slight increase in the percentage of β-sheets (13%). After the IL-based extraction step there is a similar value of α-helix (58%) content and a small increase in β-sheets (23%). β-Sheets are formed when several β-strands self-assemble, being stabilized by interstrand hydrogen bonding, and leading to the formation of extended amphipathic sheets in which hydrophobic side-chains point in one direction and polar side-chains in the other [74]. Accordingly, the application of IL-based ABSs seems to improve the self-assembling of β-strands and establishment of hydrogen-bonding interactions. Despite these small differences, which are inherently related to the media in which the protein is dissolved and interactions they face, we can conclude that the overall BSA conformation is mostly maintained, reinforcing the possibility of using appropriate IL-based ABSs for its extraction and purification from the original biological medium.

4. Conclusions

The aim of this work was the development of novel IL-based ABS as appropriate protein separation platforms and to provide a better understanding of the conditions required to apply these ABS without leading to the protein's loss of stability. The phase diagrams of all ABS investigated, composed of IL + K_2HPO_4/KH_2PO_4 buffer pH 7 + H_2O, were firstly determined at 25°C and atmospheric pressure. Then, the extraction efficiency and yield of pure BSA were evaluated for each system under study. It was found that the best ABS is constituted by [N_{4444}][Ac], allowing for extraction efficiencies and recovery yields of 100% and 84.9%, respectively. The performance of this ABS was then evaluated using real bovine serum samples, allowing for the separation of the BSA, with 85.6% of extraction yield and 61.2% of purity when a bovine serum 1:15 (*v:v*) dilution was applied. Finally, the purity increase of BSA was proved by SDS-PAGE, and its stability by circular dichroism. Overall, it is here shown that ABS composed of properly designed quaternary ammonium-based ILs should be more deeply investigated in the field of proteins separation since they provide a biocompatible environment and present a lower cost when compared with the widely studied imidazolium-based counterparts.

Supplementary Materials: The following material are available online at https://www.mdpi.com/article/10.3390/app12020707/s1, Figure S1: 1-butyl-3-methylimidazolium 2-(N-morpholino) ethanesulfonate, [C_4mim][MES], ^{1}H NMR (D_2O, 300 MHz, [ppm]): 7.49 (1H,d, J = 2.0 Hz); 7.39 (1H,d, J = 2.0 Hz); 4.16 (2H,t, J = 7.1 Hz); 3.86 (3H, s); 3,73 (4H, m); 3.10 (2H, m); 2.80 (2H, m); 2.57 (4H, m); 1.82 (2H, m); 1.29 (2H, m); 0.89 (3H, t, J = 7.4Hz), Figure S2: 1-butyl-3-methylimidazolium 2-(N-morpholino)ethanesulfonate, [C_4mim][MES], ^{13}C NMR (D_2O, 75.47 MHz, [ppm]): 123.33; 122.08; 66.09; 52.51; 52.19; 49.16; 47.25; 35.48; 31.17; 18.79; 12.64, Figure S3: Tetrabutylammonium 2-(N-morpholino)ethanesulfonate, [N_{4444}][MES], ^{1}H NMR (D_2O, 300 MHz, [ppm]): 3.77 (m, 4H); 3.178 (m, 10H); 2.843 (m, 2H); 2.61 (t, 4H); 1.66 (m, 8H); 1.38 (m, 8H); 0.96 (t, 12H). Figure S4: Tetrabutylammonium 2-(N-morpholino)ethanesulfonate, [N_{4444}][MES], ^{13}C NMR (D2O, 75.47 MHz, [ppm]): 66.02; 58.02; 52.51; 52.19; 47.25; 23.07; 19.11; 12.77. Figure S5: Tetrabutylphosphonium 2-(N-morpholino)ethanesulfonate, [P_{4444}][MES], ^{1}H NMR (D_2O, 300 MHz, [ppm]): 3.77 (m, 4H); 3.12 (m, 2H); 2.83 (m, 2H); 2.61 (t, 4H); 2.18 (m, 8H); 1.54 (m, 16H); 0.93 (t, 12H). Figure S6: Tetrabutylphosphonium 2-(N-morpholino)ethanesulfonate, [P_{4444}][MES], ^{13}C NMR (D_2O, 75.47 MHz, [ppm]): 66.09; 52.51; 52.19; 47.24; 23.35; 22.62; 17.90; 12.49. Figure S7: Tetrabutylammonium arginate, [N_{4444}][Arg], ^{1}H NMR (D_2O, 300 MHz, [ppm]): 3.21 (m, 10H); 1.68 (m, 10H); 1.36 (m, 11H); 0.96 (t, 12H). Figure S8: Tetrabutylammonium arginate, [N_{4444}][Arg], ^{13}C NMR (D_2O, 75.47 MHz, [ppm]): 180.81; 58.07; 55.51; 40.91; 31.60; 24.46; 23.05; 19.08; 12.77. Figure S9: Tetrabutylphosphonium arginate, [P_{4444}][Arg], ^{1}H NMR (D_2O, 300 MHz, [ppm]): 3.24 (m, 3H); 2.17 (t, 8H); 1.59 (m, 20H); 0.93 (t, 12H). Figure S10: Tetrabutylphosphonium arginate, [P_{4444}][Arg], ^{13}C NMR (D_2O, 75.47 MHz, [ppm]): 183.17; 55.51; 40.99; 31.63; 24.50; 23.13; 17.87; 12.48. Figure S11: Tetrabutylammonium acetate, [N_{4444}][Ac], ^{1}H NMR (D_2O, 300 MHz, [ppm]): 3.21 (t, 8H); 1.91 (s, 3H); 1.67 (m, 8H); 1.38 (m, 8H); 0.95 (t, 12H). Figure S12: Tetrabutylammonium acetate, [N_{4444}][Ac], ^{13}C NMR (D_2O, 75.47 MHz, [ppm]): 181.07; 57.99; 23.33; 23.05; 19.09; 12.82. Figure S13: Tetrabutylphosphonium acetate, [P_{4444}][Ac], ^{1}H NMR (D_2O, 300 MHz, [ppm]): ^{1}H NMR (D_2O, 300 MHz, [ppm]): 2.17 (m, 8H); 1.91 (s, 3H); 1.50 (m, 16H); 0.93 (t, 12H). Figure S14: Tetrabutylphosphonium acetate, [P_{4444}][Ac], ^{13}C NMR (D_2O, 75.47 MHz,

[ppm]): 180.83; 23.15; 22.63; 17.90; 17.26; 12.522. Table S1: Experimental weight fraction data for the binodal curves of the ABS formed by $[C_4mim][MES]$ (1) + K_2HPO_4/KH_2PO_4 (2) + H_2O (3) at (25 ± 1) °C and pH 7. Table S2: Experimental weight fraction data for the binodal curves of the ABS formed by $[N_{4444}][MES]$ (1) + K_2HPO_4/KH_2PO_4 (2) + H_2O (3) at (25 ± 1) °C and pH 7. Table S3: Experimental weight fraction for the binodal curves of the ABS formed by $[P_{4444}][MES]$ (1) + K_2HPO_4/KH_2PO_4 (2) + H_2O (3) at (25 ± 1) °C and pH 7. Table S4: Experimental weight fraction for the binodal curves of the ABS formed by $[N_{4444}][Arg]$ (1) + K_2HPO_4/KH_2PO_4 (2) + H_2O (3) at (25 ± 1) °C and pH 7. Table S5: Experimental weight fraction for the binodal curves of the ABS formed by $[P_{4444}][Arg]$ (1) + K_2HPO_4/KH_2PO_4 (2) + H_2O (3) at (25 ± 1) °C and pH 7. Table S6. Experimental weight fraction for the binodal curves of the ABS formed by $[C_4mim][Ac]$ (1) + K_2HPO_4/KH_2PO_4 (2) + H_2O (3) at (25 ± 1) °C and pH 7. Table S7. Experimental weight fraction for the binodal curves of the ABS formed by $[N_{4444}][Ac]$ (1) + K_2HPO_4/KH_2PO_4 (2) + H_2O (3) at (25 ± 1) °C and pH 7. Table S8: Experimental weight fraction for the binodal curves of the ABS formed by $[P_{4444}][Ac]$ (1) + K_2HPO_4/KH_2PO_4 (2) + H_2O (3) at (25 ± 1) °C and pH 7. Table S9: Correlation parameters of Equations (1) and (2) used to describe the experimental binodal curve of the system. Table S10: Data of TLs and TLLs for the systems composed of IL + K_2HPO_4/KH_2PO_4 buffer at pH 7 + H_2O. [IL] and [salt] represents the compositions of IL and salt, respectively and content of water corresponds to the amount required to reach 100 wt%. Figure S15: Phase diagrams for the systems composed of IL + K_2HPO_4/KH_2PO_4 buffer at pH 7 + H_2O at 25 °C: $[C_4mim][MES]$ (●); $[N_{4444}][MES]$ (⧫); $[P_{4444}][MES]$ (▲); $[N_{4444}][Arg]$ (▲); $[P_{4444}][Arg]$ (⧫); $[C_4mim][Ac]$ (⧫); $[N_{4444}][Ac]$ (■); $[P_{4444}][Ac]$ (●). Table S11: Extraction efficiencies (*EE%*) and yield of ABS composed of IL + K_2HPO_4/KH_2PO_4 pH 7 + H_2O for pure BSA. Table S12: Yield and purity of BSA from bovine serum by ABS composed of $[N_{4444}][Ac]$ + K_2HPO_4/KH_2PO_4 pH 7 + H_2O. Figure S16. SE-HPLC Chromatogram with bovine serum dilution 1:15 (*v:v*) (—-)), pure BSA 0.8 $g{\cdot}L^{-1}$ (—) and top-phase of the system $[N_{4444}][Ac]$ + K_2HPO_4/KH_2PO_4 buffer at pH 7 + bovine serum 1:15 (*v:v*) (—-).

Author Contributions: Conceptualization, M.G.F.; investigation, A.F.C.S.R., M.R.A., and M.S.; resources, J.A.P.C. and M.G.F.; writing—original draft preparation, A.F.C.S.R.; writing—review and editing, M.R.A., J.A.P.C., and M.G.F.; supervision, M.R.A., J.A.P.C., and M.G.F.; project administration, M.G.F. All authors have read and agreed to the published version of the manuscript.

Funding: This work was developed within the scope of the project CICECO-Aveiro Institute of Materials, UIDB/50011/2020 & UIDP/50011/2020, financed by national funds through the FCT/MECS. This work was developed within the scope of the project "IL2BioPro"—PTDC/BII-BBF/30840/2017—funded by FEDER, through COMPETE2020—Programa Operacional Competitividade e Internacionalização (POCI), and by national funds (OE), through FCT/MCTES. A.F.C.S. Rufino acknowledge FCT for the PhD grant SFRH/BD/138997/2018.

Institutional Review Board Statement: Not applicable.

Informed Consent Statement: Not applicable.

Data Availability Statement: Data are contained within the article or Supplementary Material.

Conflicts of Interest: The authors declare no conflict of interest.

References

1. Wong, F.W.F.; Ariff, A.B.; Stuckey, D.C. Downstream protein separation by surfactant precipitation: A review. *Crit. Rev. Biotechnol.* **2018**, *38*, 31–46. [CrossRef] [PubMed]
2. Ayyar, B.V.; Arora, S.; Murphy, C.; O'Kennedy, R. Affinity chromatography as a tool for antibody purification. *Methods* **2012**, *56*, 116–129. [CrossRef] [PubMed]
3. Berg, J.M.; Tymoczko, J.L.; Stryer, L. *Biochemistry*, 5th ed.; W.H. Freeman and Company: New York, NY, USA, 2002.
4. Ribeiro, S.C.; Monteiro, G.A.; Cabral, J.M.S.; Prazeres, D.M.F. Isolation of plasmid DNA from cell lysates by aqueous two-phase systems. *Biotechnol. Bioeng.* **2002**, *78*, 376–384. [CrossRef] [PubMed]
5. Almeida, M.R.; Passos, H.; Pereira, M.M.; Lima, Á.S.; Coutinho, J.A.P.; Freire, M.G. Ionic liquids as additives to enhance the extraction of antioxidants in aqueous two-phase systems. *Sep. Purif. Technol.* **2014**, *128*, 1–10. [CrossRef]
6. Cabral, J.M.S. Cell Partitioning in Aqueous Two-Phase Polymer Systems. In *Cell Separation*; Springer: Berlin/Heidelberg, Germany, 2007; pp. 151–171.
7. Frerix, A.; Müller, M.; Kula, M.; Hubbuch, J. Scalable recovery of plasmid DNA based on aqueous two-phase separation. *Biotechnol. Appl. Biochem.* **2005**, *42*, 57–66. [PubMed]

8. Wysoczanska, K.; Do, H.T.; Held, C.; Sadowski, G.; Macedo, E.A. Effect of different organic salts on amino acids partition behaviour in PEG-salt ATPS. *Fluid Phase Equilib.* **2018**, *456*, 84–91. [CrossRef]
9. Rosa, P.A.J.; Azevedo, A.M.; Ferreira, I.F.; De Vries, J.; Korporaal, R.; Verhoef, H.J.; Visser, T.J.; Aires-Barros, M.R. Affinity partitioning of human antibodies in aqueous two-phase systems. *J. Chromatogr. A* **2007**, *1162*, 103–113. [CrossRef]
10. Iqbal, M.; Tao, Y.; Xie, S.; Zhu, Y.; Chen, D.; Wang, X.; Huang, L.; Peng, D.; Sattar, A.; Shabbir, M.A.B. Aqueous two-phase system (ATPS): An overview and advances in its applications. *Biol. Proced. Online* **2016**, *18*, 1–8. [CrossRef] [PubMed]
11. Torres-Acosta, M.A.; Pereira, J.F.B.; Freire, M.G.; Aguilar-Yáñez, J.M.; Coutinho, J.A.P.; Titchener-Hooker, N.J.; Rito-Palomares, M. Economic evaluation of the primary recovery of tetracycline with traditional and novel aqueous two-phase systems. *Sep. Purif. Technol.* **2018**, *203*, 178–184. [CrossRef] [PubMed]
12. Silvério, S.C.; Rodríguez, O.; Tavares, A.P.M.; Teixeira, J.A.; Macedo, E.A. Laccase recovery with aqueous two-phase systems: Enzyme partitioning and stability. *J. Mol. Catal. B Enzym.* **2013**, *87*, 37–43. [CrossRef]
13. Freire, M.G.; Claudio, A.F.M.; Araujo, J.M.M.; Coutinho, J.A.P.; Marrucho, I.M.; Lopes, J.N.C.; Rebelo, L.P.N. Aqueous biphasic systems: A boost brought about by using ionic liquids. *Chem. Soc. Rev.* **2012**, *41*, 4966–4995. [CrossRef]
14. Gutowski, K.E.; Broker, G.A.; Willauer, H.D.; Huddleston, J.G.; Swatloski, R.P.; Holbrey, J.D.; Rogers, R.D. Controlling the aqueous miscibility of ionic liquids: Aqueous biphasic systems of water-miscible ionic liquids and water-structuring salts for recycle, metathesis, and separations. *J. Am. Chem. Soc.* **2003**, *125*, 6632–6633. [CrossRef] [PubMed]
15. Pereira, J.F.B.; Lima, Á.S.; Freire, M.G.; Coutinho, J.A.P. Ionic liquids as adjuvants for the tailored extraction of biomolecules in aqueous biphasic systems. *Green Chem.* **2010**, *12*, 1661–1669. [CrossRef]
16. Pereira, J.F.B.; Rebelo, L.P.N.; Rogers, R.D.; Coutinho, J.A.P.; Freire, M.G. Combining ionic liquids and polyethylene glycols to boost the hydrophobic–hydrophilic range of aqueous biphasic systems. *Phys. Chem. Chem. Phys.* **2013**, *15*, 19580–19583. [CrossRef] [PubMed]
17. Taha, M.; e Silva, F.A.; Quental, M.V.; Ventura, S.P.M.; Freire, M.G.; Coutinho, J.A.P. Good's buffers as a basis for developing self-buffering and biocompatible ionic liquids for biological research. *Green Chem.* **2014**, *16*, 3149–3159. [CrossRef] [PubMed]
18. Taha, M.; Quental, M.V.; Correia, I.; Freire, M.G.; Coutinho, J.A.P. Extraction and stability of bovine serum albumin (BSA) using cholinium-based Good's buffers ionic liquids. *Process Biochem.* **2015**, *50*, 1158–1166. [CrossRef]
19. Taha, M.; Quental, M.V.; e Silva, F.A.; Capela, E.V.; Freire, M.G.; Ventura, S.P.M.; Coutinho, J.A.P. Good's buffer ionic liquids as relevant phase-forming components of self-buffered aqueous biphasic systems. *J. Chem. Technol. Biotechnol.* **2017**, *92*, 2287–2299. [CrossRef]
20. Tang, F.; Zhang, Q.; Ren, D.; Nie, Z.; Liu, Q.; Yao, S. Functional amino acid ionic liquids as solvent and selector in chiral extraction. *J. Chromatogr. A* **2010**, *1217*, 4669–4674. [CrossRef]
21. Li, Z.; Liu, X.; Pei, Y.; Wang, J.; He, M. Design of environmentally friendly ionic liquid aqueous two-phase systems for the efficient and high activity extraction of proteins. *Green Chem.* **2012**, *14*, 2941–2950. [CrossRef]
22. Deive, F.J.; Rodríguez, A.; Rebelo, L.P.N.; Marrucho, I.M. Extraction of Candida antarctica lipase A from aqueous solutions using imidazolium-based ionic liquids. *Sep. Purif. Technol.* **2012**, *97*, 205–210. [CrossRef]
23. Du, Z.; Yu, Y.; Wang, J. Extraction of proteins from biological fluids by use of an ionic liquid/aqueous two-phase system. *Chem. Eur. J.* **2007**, *13*, 2130–2137. [CrossRef] [PubMed]
24. Belchior, D.C.V.; Quental, M.V.; Pereira, M.M.; Mendonça, C.M.N.; Duarte, I.F.; Freire, M.G. Performance of tetraalkylammonium-based ionic liquids as constituents of aqueous biphasic systems in the extraction of ovalbumin and lysozyme. *Sep. Purif. Technol.* **2020**, *233*, 116019. [CrossRef]
25. Akdogan, Y.; Emrullahoglu, M.; Tatlidil, D.; Ucuncu, M.; Cakan-Akdogan, G. EPR studies of intermolecular interactions and competitive binding of drugs in a drug–BSA binding model. *Phys. Chem. Chem. Phys.* **2016**, *18*, 22531–22539. [CrossRef] [PubMed]
26. Lang, X.-D.; Zhang, S.; Song, Q.-W.; He, L.-N. Tetra-butylphosphonium arginine-based ionic liquid-promoted cyclization of 2-aminobenzonitrile with carbon dioxide. *RSC Adv.* **2015**, *5*, 15668–15673. [CrossRef]
27. Carreira, A.R.F.; Rocha, S.N.; e Silva, F.A.; Sintra, T.E.; Passos, H.; Ventura, S.P.M.; Coutinho, J.A.P. Amino-acid-based chiral ionic liquids characterization and application in aqueous biphasic systems. *Fluid Phase Equilib.* **2021**, *542*, 113091. [CrossRef]
28. Ventura, S.P.M.; Sousa, S.G.; Serafim, L.S.; Lima, Á.S.; Freire, M.G.; Coutinho, J.A.P. Ionic liquid based aqueous biphasic systems with controlled pH: The ionic liquid cation effect. *J. Chem. Eng. Data* **2011**, *56*, 4253–4260. [CrossRef]
29. Mourão, T.; Cláudio, A.F.M.; Boal-Palheiros, I.; Freire, M.G.; Coutinho, J.A.P. Evaluation of the impact of phosphate salts on the formation of ionic-liquid-based aqueous biphasic systems. *J. Chem. Thermodyn.* **2012**, *54*, 398–405. [CrossRef]
30. Merchuk, J.C.; Andrews, B.A.; Asenjo, J.A. Aqueous two-phase systems for protein separation: Studies on phase inversion. *J. Chromatogr. B Biomed. Sci. Appl.* **1998**, *711*, 285–293. [CrossRef]
31. Miles, A.J.; Ramalli, S.G.; Wallace, B.A. DichroWeb, a website for calculating protein secondary structure from circular dichroism spectroscopic data. *Protein Sci.* **2021**, *31*, 37–46. [CrossRef]
32. Louros, C.L.S.; Cláudio, A.F.M.; Neves, C.M.S.S.; Freire, M.G.; Marrucho, I.M.; Pauly, J.; Coutinho, J.A.P. Extraction of biomolecules using phosphonium-based ionic liquids + K3PO4 aqueous biphasic systems. *Int. J. Mol. Sci.* **2010**, *11*, 1777–1791. [CrossRef]
33. Bridges, N.J.; Gutowski, K.E.; Rogers, R.D. Investigation of aqueous biphasic systems formed from solutions of chaotropic salts with kosmotropic salts (salt–salt ABS). *Green Chem.* **2007**, *9*, 177–183. [CrossRef]
34. Dreyer, S.; Kragl, U. Ionic liquids for aqueous two-phase extraction and stabilization of enzymes. *Biotechnol. Bioeng.* **2008**, *99*, 1416–1424. [CrossRef] [PubMed]

35. Oppermann, S.; Stein, F.; Kragl, U. Ionic liquids for two-phase systems and their application for purification, extraction and biocatalysis. *Appl. Microbiol. Biotechnol.* **2011**, *89*, 493–499. [CrossRef] [PubMed]
36. Lee, S.Y.; Khoiroh, I.; Ooi, C.W.; Ling, T.C.; Show, P.L. Recent advances in protein extraction using ionic liquid-based aqueous two-phase systems. *Sep. Purif. Rev.* **2017**, *46*, 291–304. [CrossRef]
37. Nunes, J.C.F.; Almeida, M.R.; Faria, J.L.; Silva, C.G.; Neves, M.C.; Freire, M.G.; Tavares, A.P.M. Overview on Protein Extraction and Purification Using Ionic-Liquid-Based Processes. *J. Solut. Chem.* **2021**, *50*, 1–36. [CrossRef]
38. Dreyer, S.; Salim, P.; Kragl, U. Driving forces of protein partitioning in an ionic liquid-based aqueous two-phase system. *Biochem. Eng. J.* **2009**, *46*, 176–185. [CrossRef]
39. Pei, Y.; Wang, J.; Wu, K.; Xuan, X.; Lu, X. Ionic liquid-based aqueous two-phase extraction of selected proteins. *Sep. Purif. Technol.* **2009**, *64*, 288–295. [CrossRef]
40. Chen, J.; Wang, Y.; Zeng, Q.; Ding, X.; Huang, Y. Partition of proteins with extraction in aqueous two-phase system by hydroxyl ammonium-based ionic liquid. *Anal. Methods* **2014**, *6*, 4067–4076. [CrossRef]
41. Raja, S.; Murty, V.R. Development and evaluation of environmentally benign aqueous two phase systems for the recovery of proteins from tannery waste water. *ISRN Chem. Eng.* **2012**, *2012*, 1–9. [CrossRef]
42. Chaiyasut, C.; Tsuda, T. Isoelectric points estimation of proteins by electroosmotic flow: pH relationship using physically adsorbed proteins on silica gel. *Chromatography* **2001**, *22*, 91–96.
43. Shu, Y.; Liu, M.; Chen, S.; Chen, X.; Wang, J. New insight into molecular interactions of imidazolium ionic liquids with bovine serum albumin. *J. Phys. Chem. B* **2011**, *115*, 12306–12314. [CrossRef]
44. Attri, P.; Venkatesu, P. Ammonium ionic liquids as convenient co-solvents for the structure and stability of succinylated Con A. *J. Chem. Thermodyn.* **2012**, *52*, 78–88. [CrossRef]
45. Zafarani-Moattar, M.T.; Shekaari, H.; Jafari, P. Thermodynamic study of aqueous two-phase systems containing biocompatible cholinium aminoate ionic-liquids and polyethylene glycol di-methyl ether 250 and their performances for bovine serum albumin separation. *J. Chem. Thermodyn.* **2019**, *130*, 17–32. [CrossRef]
46. Pereira, M.M.; Pedro, S.N.; Quental, M.V.; Lima, Á.S.; Coutinho, J.A.P.; Freire, M.G. Enhanced extraction of bovine serum albumin with aqueous biphasic systems of phosphonium-and ammonium-based ionic liquids. *J. Biotechnol.* **2015**, *206*, 17–25. [CrossRef] [PubMed]
47. Zafarani-Moattar, M.T.; Shekaari, H.; Jafari, P. Structural effects of choline amino acid ionic liquids on the extraction of bovine serum albumin by green and biocompatible aqueous biphasic systems composed of polypropylene glycol400 and choline amino acid ionic liquids. *J. Mol. Liq.* **2020**, *301*, 112397. [CrossRef]
48. Zafarani-Moattar, M.T.; Shekaari, H.; Jafari, P. Design of Novel Biocompatible and Green Aqueous two-Phase Systems containing Cholinium L-alaninate ionic liquid and polyethylene glycol di-methyl ether 250 or polypropylene glycol 400 for separation of bovine serum albumin (BSA). *J. Mol. Liq.* **2018**, *254*, 322–332. [CrossRef]
49. Pei, Y.; Li, Z.; Liu, L.; Wang, J.; Wang, H. Selective separation of protein and saccharides by ionic liquids aqueous two-phase systems. *Sci. China Chem.* **2010**, *53*, 1554–1560. [CrossRef]
50. Schröder, C. Proteins in Ionic Liquids: Current Status of Experiments and Simulations. In *Ionic Liquids II*; Springer: Berlin/Heidelberg, Germany, 2017; pp. 127–152.
51. Fujita, K.; MacFarlane, D.R.; Forsyth, M. Protein solubilising and stabilising ionic liquids. *Chem. Commun.* **2005**, *38*, 4804–4806. [CrossRef]
52. Haberler, M.; Schröder, C.; Steinhauser, O. Hydrated ionic liquids with and without solute: The influence of water content and protein solutes. *J. Chem. Theory Comput.* **2012**, *8*, 3911–3928. [CrossRef]
53. Klähn, M.; Lim, G.S.; Seduraman, A.; Wu, P. On the different roles of anions and cations in the solvation of enzymes in ionic liquids. *Phys. Chem. Chem. Phys.* **2011**, *13*, 1649–1662. [CrossRef]
54. Egorov, V.M.; Smirnova, S.V.; Pletnev, I.V. Highly efficient extraction of phenols and aromatic amines into novel ionic liquids incorporating quaternary ammonium cation. *Sep. Purif. Technol.* **2008**, *63*, 710–715. [CrossRef]
55. Stepnowski, P.; Skladanowski, A.C.; Ludwiczak, A.; Laczyńska, E. Evaluating the cytotoxicity of ionic liquids using human cell line HeLa. *Hum. Exp. Toxicol.* **2004**, *23*, 513–517. [CrossRef] [PubMed]
56. Stolte, S.; Abdulkarim, S.; Arning, J.; Blomeyer-Nienstedt, A.-K.; Bottin-Weber, U.; Matzke, M.; Ranke, J.; Jastorff, B.; Thöming, J. Primary biodegradation of ionic liquid cations, identification of degradation products of 1-methyl-3-octylimidazolium chloride and electrochemical wastewater treatment of poorly biodegradable compounds. *Green Chem.* **2008**, *10*, 214–224. [CrossRef]
57. Cohn, E.J.; Strong, L.E.; Hughes, W.; Mulford, D.J.; Ashworth, J.N.; Melin, M.E.; Taylor, H.L. Preparation and Properties of Serum and Plasma Proteins. IV. A System for the Separation into Fractions of the Protein and Lipoprotein Components of Biological Tissues and Fluids 1a,b,c,d. *J. Am. Chem. Soc.* **1946**, *68*, 459–475. [CrossRef]
58. Cohn, E.J.; Gurd, F.R.N.; Surgenor, D.M.; Barnes, B.A.; Brown, R.K.; Derouaux, G.; Gillespie, J.M.; Kahnt, F.W.; Lever, W.F.; Liu, C.H. A system for the separation of the components of human blood: Quantitative procedures for the separation of the protein components of human plasma1a, b, c. *J. Am. Chem. Soc.* **1950**, *72*, 465–474. [CrossRef]
59. Johnston, A.; Adcock, W. The use of chromatography to manufacture purer and safer plasma products. *Biotechnol. Genet. Eng. Rev.* **2000**, *17*, 37–70. [CrossRef]

60. Tanaka, K.; Shigueoka, E.M.; Sawatani, E.; Dias, G.A.; Arashiro, F.; Campos, T.; Nakao, H.C. Purification of human albumin by the combination of the method of Cohn with liquid chromatography. *Braz. J. Med. Biol. Res.* **1998**, *31*, 1383–1388. [CrossRef] [PubMed]
61. Raoufinia, R.; Mota, A.; Keyhanvar, N.; Safari, F.; Shamekhi, S.; Abdolalizadeh, J. Overview of albumin and its purification methods. *Adv. Pharm. Bull.* **2016**, *6*, 495. [CrossRef]
62. Odunuga, O.O.; Shazhko, A. Ammonium sulfate precipitation combined with liquid chromatography is sufficient for purification of bovine serum albumin that is suitable for most routine laboratory applications. *Biochemical Compounds Comp.* **2013**, *1*, 1–6. [CrossRef]
63. Vasileva, R.; Jakab, M.; Hasko, F. Application of ion-exchange chromatography for the production of human albumin. *J. Chromatogr. A* **1981**, *216*, 279–284. [CrossRef]
64. Denizli, A.; Pişkin, E. Dye-ligand affinity systems. *J. Biochem. Biophys. Methods* **2001**, *49*, 391–416. [CrossRef]
65. Balkani, S.; Shamekhi, S.; Raoufinia, R.; Parvan, R.; Abdolalizadeh, J. Purification and characterization of bovine serum albumin using chromatographic method. *Adv. Pharm. Bull.* **2016**, *6*, 651. [CrossRef] [PubMed]
66. Imamoglu, S. Simulated Moving Bed Chromatography (SMB) for Application in Bioseparation. In *Modern Advances in Chromatography*; Springer: Berlin/Heidelberg, Germany, 2002; pp. 211–231.
67. Wang, C.; Bai, S.; Tao, S.-P.; Sun, Y. Evaluation of steric exclusion chromatography on cryogel column for the separation of serum proteins. *J. Chromatogr. A* **2014**, *1333*, 54–59. [CrossRef] [PubMed]
68. Soares, B.P.; Santos, J.H.P.M.; Martins, M.; Almeida, M.R.; Santos, N.V.; Freire, M.G.; Santos-Ebinuma, V.C.; Coutinho, J.A.P.; Pereira, J.F.B.; Ventura, S.P.M. Purification of green fluorescent protein using fast centrifugal partition chromatography. *Sep. Purif. Technol.* **2021**, *257*, 117648. [CrossRef]
69. Capela, E.V.; Santiago, A.E.; Rufino, A.F.C.S.; Tavares, A.P.M.; Pereira, M.M.; Mohamadou, A.; Aires-Barros, M.R.; Coutinho, J.A.P.; Azevedo, A.M.; Freire, M.G. Sustainable strategies based on glycine–betaine analogue ionic liquids for the recovery of monoclonal antibodies from cell culture supernatants. *Green Chem.* **2019**, *21*, 5671–5682. [CrossRef]
70. Kelly, S.M.; Jess, T.J.; Price, N.C. How to study proteins by circular dichroism. *Biochim. Biophys. Acta (BBA)-Proteins Proteom.* **2005**, *1751*, 119–139. [CrossRef]
71. Güler, G.; Vorob'ev, M.M.; Vogel, V.; Mäntele, W. Proteolytically-induced changes of secondary structural protein conformation of bovine serum albumin monitored by Fourier transform infrared (FT-IR) and UV-circular dichroism spectroscopy. *Spectrochim. Acta Part A Mol. Biomol. Spectrosc.* **2016**, *161*, 8–18. [CrossRef]
72. Charbonneau, D.M.; Tajmir-Riahi, H.-A. Study on the interaction of cationic lipids with bovine serum albumin. *J. Phys. Chem. B* **2010**, *114*, 1148–1155. [CrossRef]
73. Tian, J.; Liu, J.; Hu, Z.; Chen, X. Binding of the scutellarin to albumin using tryptophan fluorescence quenching, CD and FT-IR spectra. *Am. J. Immunol.* **2005**, *1*, 21–23. [CrossRef]
74. Boyle, A.L. Applications of de novo designed peptides. In *Peptide Applications in Biomedicine, Biotechnology and Bioengineering*; Elsevier: Amsterdam, The Netherlands, 2018; pp. 51–86.